

Integrated Data-driven Inference and Planning-based Human Motion Prediction for Safe Human-Robot Interaction

Youngim Nam and Cheolhyeon Kwon

Abstract—This paper presents a unified prediction and planning algorithm for an autonomous vehicle to interact with an uncertain human-driven vehicle. Predicting human motion is challenging due to inherent uncertainties in diverse human internal states, i.e., driving styles and rationality. To address these complexities, we propose a hierarchical prediction strategy that combines data-driven internal state inference and planning-based human motion prediction. First, we employ Long Short Term Memory Networks (LSTM) based inference modules to capture both driving styles and rationality from the observed motion of human driver. With these inferred internal states, we predict the future trajectories of human-driven vehicle by formulating a human planning model as an optimization problem. Lastly, we present a Stochastic Model Predictive Control (SMPC) for the autonomous vehicle to safely interact with the human-driven vehicle while actively inferring human internal states. The simulation results, demonstrating the lane change scenarios, indicate the proposed method outperforms the existing work in both predicting the human motion and achieving the robot’s goal.

I. INTRODUCTION

Over the last few decades, autonomous driving technologies have made significant advancements in operating under diverse traffic conditions. Among these, safe Human-Robot Interaction (HRI) is a key enabler when the autonomous vehicle is situated in human-driven vehicle combined traffic. This task, however, presents a formidable challenge, as it necessitates the capability to account for a multitude of uncertainties inherent in predicting human motion. In considering these challenges, existing research on motion prediction can be broadly classified into two main approaches [1]: (1) data-driven methods and (2) model-based methods.

In data-driven approaches, a wide range of machine learning techniques has been proposed, encompassing classification algorithms designed to discern human intents [2], [3], [4], as well as regression or generative models that directly output the plausible human trajectories [5], [6]. Nevertheless, the precision and adaptability of data-driven models hinge on the volume and representativeness of training data, rendering them vulnerable to data scarcity in less common or perilous scenarios. Furthermore, human decision-making is intrinsically influenced by individual *internal states*, such as driving styles and rationality. Consequently, purely data-

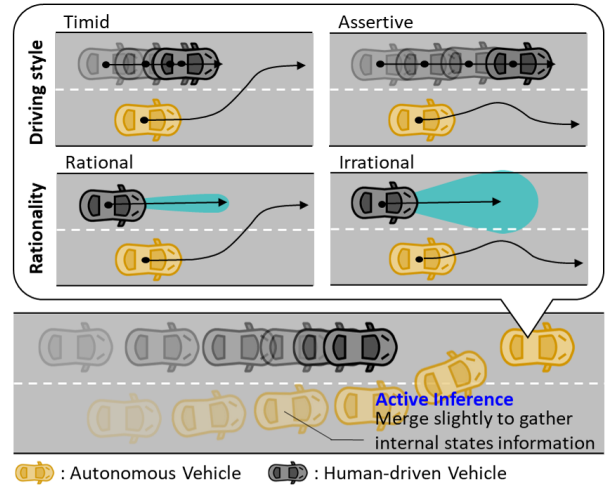


Fig. 1. Safe interaction with a human-driven vehicle exhibiting uncertain internal states: driving styles (e.g., timid/assertive) and rationality (e.g., rational/irrational).

driven approaches may struggle to explicitly express the nuanced aspects of human motion.

In the model-based approach, the straightforward prediction strategy represents humans through simplified physics-based models. These approaches facilitate predictions using traditional statistical tools like Kalman filter [7]. Nevertheless, these methods may lack reliability when it comes to long-term predictions because of their restricted capacity to capture complex human motions. To enhance the prediction capabilities regarding human motion, a new advanced model-based approach is a planning-based method, which models the human decision-making process as an optimization problem [8], [9]. These approaches assume that humans strategically select motions to optimize their own rewards. This aspect enables the integration of human internal states within the human reward function, allowing the model to systemically reason out the predicted human motion.

In reality, there can be differences in the internal states of individuals and cannot be directly measured by sensor observations. Consequently, the autonomous vehicle faces the imperative task of inferring these internal states in real time. To address this challenge, Bayesian estimation has been proposed to compute the belief over probable internal states [10], but they become complex in high-dimensional state spaces. Furthermore, the majority of existing research relies on passive observation, often resulting in deficient internal state information for precise predictions. To overcome this,

*This work was supported by the National Research Foundation of Korea (NRF) Grants funded by the Korea Government (MSIT) under Grant 2020R1A5A8018822, and in part by the 2023 Research Fund (1.230024.01) of Ulsan National Institute of Science and Technology (UNIST).

The authors are with the Department of Mechanical Engineering, Ulsan National Institute of Science and Technology, Ulsan, 44919, Republic of Korea (e-mail:nyi0944@unist.ac.kr;kwonc@unist.ac.kr)

an active inference strategy has been proposed to expedite the prediction through the autonomous vehicle’s motion planning [11], [12]. Still, most active inference work does not sufficiently consider human rationality, leaving it susceptible to safety concerns posed by irrational human motion.

Motivated by the aforementioned challenges, we propose a novel prediction and planning algorithm for an autonomous vehicle to safely and actively interact with an uncertain human-driven vehicle (See Fig. 1). The proposed algorithm establishes a hierarchical strategy that seamlessly combines a data-driven approach with a planning-based approach to carry out both precision and expressivity of human motion prediction. We first develop LSTM-based inference modules [13] to deal with uncertain human internal states, i.e., driving styles and rationality. The proposed algorithm leverages the data-driven approach to tackle the continuous level of human rationality without necessitating prior domain expertise in the complex probability structures of internal states.

Second, our algorithm predicts future human motions based on the inferred internal states. We assume that humans choose their motions to maximize their expected rewards according to the inferred driving style, and further adjust based on the inferred rationality. Finally, under this probability distribution, the motion planning for the autonomous vehicle is formalized as a sampling-based SMPC problem. This formulation successfully conforms to the HRI task for the autonomous vehicle such that not only ensures safety against the uncertain human motion but also actively gathers information on the human internal states.

The main contributions of this paper are summarized as follows:

- A hierarchical prediction strategy that integrates data-driven human internal state inference with planning-based human motion prediction;
- A computationally affordable motion planning algorithm for the autonomous vehicle to ensure safety against uncertain human motions while actively inferring the human internal states; and
- Comparative analysis to evaluate the effectiveness of the proposed method in the context of lane changing scenario;

II. RELATED WORK

One common approach to predicting human motion is the planning-based approach, where human motion is decided to maximize its own reward functions [14]. In characterizing the human reward function, previous research has focused on the Inverse Reinforcement Learning (IRL) approach [15]. In IRL, the reward function is formulated as a linear combination of potential features, with their associated weights trained to represent human internal states [16], [17]. However, individual humans may exhibit varying internal states, and the autonomous vehicle cannot directly observe them.

To infer human internal states online, Bayesian estimation has been proposed to compute beliefs regarding probable internal states based on observed human motions [10], [18]. However, Bayesian estimation may encounter challenges,

primarily stemming from the need for precise prior probabilities and likelihood models, particularly when dealing with high-dimensional and diverse internal states. In many instances, researchers have resorted to discretizing internal states as a simplification strategy [19], [20], but this approach may not fully capture the intricate complexity of human motion.

Additionally, a significant limitation of most inference methods is their reliance solely on passive observation, lacking the ability to support prediction through active planning. In response to this specific limitation, active inference methods have been proposed to effectively infer human internal states [21]. [11], [20] have utilized the autonomous vehicle’s reward function to decrease future entropy regarding human internal states. Alternatively, [12] has proposed the dual SMPC method to implicitly derive the active information-gathering motion of autonomous vehicle which reduces the uncertainty about the human internal state. Despite these advancements, these approaches do not sufficiently consider irrational humans whose motions erratically deviate from their own driving style.

On the other hand, recent developments in the spotlight involve the fusion of data-driven approaches with model-based approaches [22], [23]. Albeit the data-driven approaches excel at implicitly capturing human motions without extensive domain knowledge, they may fail to explicitly reason out the prediction result, potentially introducing risks when confronted with corner cases. To address this issue, some researchers have adopted the data-driven approach for limited use, such as inferring the intent of the motion, and utilized dynamic models to forecast the full motion trajectories [24], [25]. Nevertheless, even when humans share similar intents, their motions may exhibit significant variations due to different internal states. Additionally, it is worth noting that these approaches do not incorporate active inference strategies. In this paper, we introduce a method that addresses the aforementioned limitations through a unified framework for human motion prediction and active motion planning of autonomous vehicles.

III. PROBLEM FORMULATION

A. Interaction Dynamics

This paper focuses on the interaction between a single autonomous vehicle and a single human-driven vehicle. Throughout the entire paper, we denote the variables of the autonomous vehicle as $(\bullet)_r$ and the human-driven vehicle as $(\bullet)_h$, respectively. The dynamics of both vehicles are modeled using the kinematic bicycle model [26]. The vehicle state vector, represented as $x_i := [p_{x,i}, p_{y,i}, \Psi_i, v_i] \in \mathbb{R}^4$, encompasses the x-y position, heading angle, and velocity of the vehicle, respectively. The input vector is denoted as $u_i := [a_i, \delta_i] \in \mathbb{R}^2$, $i \in \{r, h\}$, where a_i denotes acceleration, and δ_i represents the steering angle. Then, the joint nonlinear dynamics of the human and autonomous vehicle is described as:

$$x(t+1) = f(x(t), u_r(t), u_h(t)) \quad (1)$$

Here, f is the interaction dynamics function, and $x(t) \in \mathbb{R}^8$ is the whole state of a human-autonomous vehicle system at time step $t \in \mathbb{N}_+$.

B. Human Decision Model

To achieve safe autonomous driving, it is essential to predict the future motion of human-driven vehicles. We assume that humans follow a noisily rational model [27] based on two internal states, i.e., driving style and rationality. According to this model, they are probabilistically choose motions that maximize their expected rewards as follows:

$$\begin{aligned} u_h(t) &\sim P(u_h(t)|x(t), u_r(t), \psi, \beta) \\ &= \frac{\exp(\beta R_h^\psi(x(t), u_r(t), u_h(t)))}{\int \exp(\beta R_h^\psi(x(t), u_r(t), \tilde{u}_h(t))) d\tilde{u}_h} \end{aligned} \quad (2)$$

where $R_h^\psi(x(t), u_r(t), u_h(t))$ represents the human reward function, which can be designed differently according to distinct driving style $\psi \in \{\psi_1, \dots, \psi_{n_\psi}\}$. Additionally, the level of rationality of humans is determined by the rationality coefficient $\beta \in (0, \infty)$. This coefficient accounts for uncertainty in human motion. As β approaches infinity, it signifies that the human exhibits perfect rationality, while as β tends towards zero, it suggests that the human acts irrationally, following uniformly random motions.

C. Motion Planning of Autonomous Vehicle

The main goal of the autonomous vehicle is to safely achieve its driving goal under the uncertainty of human motion. For brevity, we represent the predicted state and input sequences over a receding horizon of length N as $\mathbf{x} = [x^0, \dots, x^{N-1}]$ and $\mathbf{u}_i = [u_i^0, \dots, u_i^{N-1}]$ where $i \in \{r, h\}$, respectively. Given the current state $x(t)$ at time step t , we can design that the autonomous vehicle decides optimal input sequences \mathbf{u}_r^* minimizing cost using the following SMPC problem:

$$\min_{\mathbf{u}_r^*} \mathbb{E}_{u_h^k} R_r(\mathbf{x}, \mathbf{u}_r, \mathbf{u}_h) \quad (3a)$$

$$\text{s.t. } x^0 = x(t) \quad (3b)$$

$$x^{k+1} = f(x^k, u_r^k, u_h^k) \quad (3c)$$

$$u_h^k \sim P(u_h^k | x^k, u_r^k, \psi, \beta) \quad (3d)$$

$$g(x^k, u_r^k, u_h^k) \leq 0 \quad (3e)$$

$$h(x^k) \geq 0, \quad \forall k = 0, \dots, N-1 \quad (3f)$$

where $R_r(\mathbf{x}, \mathbf{u}_r, \mathbf{u}_h) := \sum_{k=0}^{N-1} r_r(x^k, u_r^k, u_h^k)$ represents the autonomous vehicle's cumulative reward over the receding horizon. Eq.(3e) is the state and input constraint for both vehicles, and Eq.(3f) corresponds to the collision avoidance constraint. This constraint is designed to ensure safety with an elliptical boundary [28]:

$$\begin{aligned} h(x^k) &= \frac{((p_{x,r}^k - p_{x,h}^k) \cos(\Psi_h^k) + (p_{y,r}^k - p_{y,h}^k) \sin(\Psi_h^k))^2}{(D_{lon}^k)^2} \\ &+ \frac{((p_{x,r}^k - p_{x,h}^k) \sin(\Psi_h^k) - (p_{y,r}^k - p_{y,h}^k) \cos(\Psi_h^k))^2}{(D_{lat}^k)^2} - 1. \end{aligned}$$

Here, D_{lon}^k and D_{lat}^k represent the axes of the ellipses to account for uncertainty in human motion (3d). Based on the initial values \bar{D}_{lon} and \bar{D}_{lat} , these parameters are computed by:

$$\begin{bmatrix} D_{lon}^k \\ D_{lat}^k \end{bmatrix} = \epsilon \begin{bmatrix} \sqrt{\Sigma_{lon}^k} \\ \sqrt{\Sigma_{lat}^k} \end{bmatrix} + \begin{bmatrix} \bar{D}_{lon} \\ \bar{D}_{lat} \end{bmatrix} \quad (4)$$

where Σ_{lon}^k and Σ_{lat}^k denote the covariance associated with the predicted position of the human-driven vehicle in its longitudinal and lateral directions, respectively. The parameter $\epsilon > 0$ is employed to fine-tune the safety boundary, taking into account our level of confidence in the estimated uncertainty. However, it is important to note that computing Eq.(3d) is intractable due to uncertain ψ and β , and thus it is necessary for the autonomous vehicle to infer them online from the observed human motion.

IV. ALGORITHM DEVELOPMENT

The proposed algorithm is decomposed into three main modules: (1) data-driven human internal state inference; (2) planning-based human motion prediction; and (3) active motion planning of autonomous vehicle. We employ two LSTM-based inference modules to respectively capture driving styles and rationality. Upon observing human motion and inferring internal states, the probability distribution of human motion is accordingly computed. Lastly, using this probability distribution, we solve the sampling-based SMPC problem. This serves the dual purpose of achieving autonomous driving goals and actively inferring human internal states. The architectural overview of our proposed algorithm is illustrated in Fig. 2.

A. Data-driven Human Internal State Inference

To perform online inference of human internal states, we employ a pair of LSTM-based inference modules. These learning networks work in tandem to capture the relationships between online observed past trajectories and internal states. Each past trajectory consists of two features at every time step: $I = \{x(i), u_h(i)\}_{i=t-N_{seq}}^t$ where N_{seq} represents the number of sequential segments that compose the past trajectory. During the training phase, we utilize datasets denoted as D_{train} , which contain data from N_D different scenarios. The data for each scenario comprises tuples $(x(i), u_h(i), \psi, \beta)_{i=0}^{N_{sim}-1}$ collected over a simulation time of length N_{sim} ¹. The training process for the two inference modules is illustrated in Fig. 3 and can be summarized as follows:

Driving Style Inference Module: We extract the past trajectories $\{x(i), u_h(i)\}_{i=t-N_{seq}}^t$ as input and label them with ψ from the D_{train} datasets for all $t = N_{seq}, \dots, N_{sim} - 1$. Subsequently, to capture the intricate relationships within these historical trajectories, we employ an LSTM layer,

¹It is worth noting that for real-world datasets, the direct access to internal states may not be feasible. In such cases, different statistical learning methods such as clustering [29] or IRL [16] can be employed to encode the human internal state.

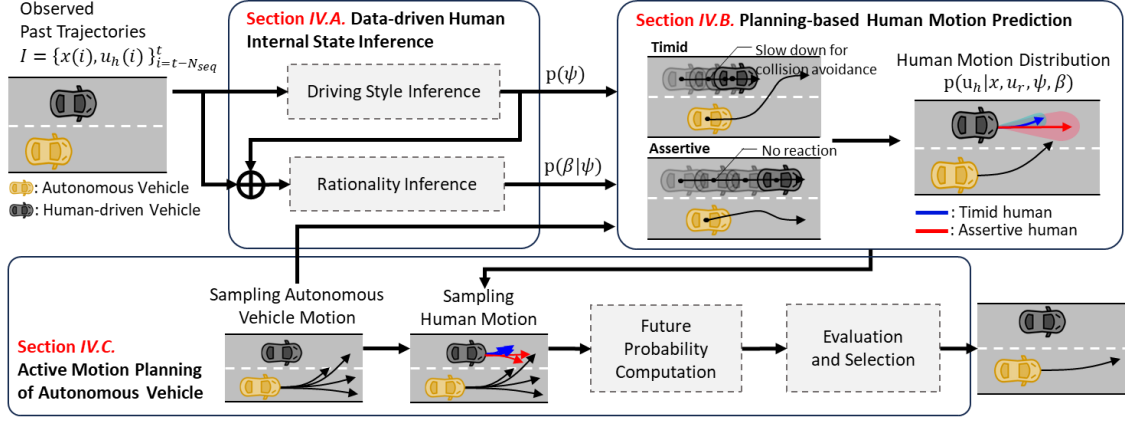


Fig. 2. The overview of the proposed algorithm: the unified framework for human motion prediction and active motion planning of autonomous vehicle.

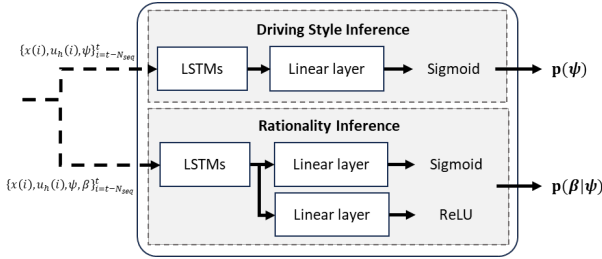


Fig. 3. The training process of the LSTM-based inference modules.

which effectively encodes the information at each state. The final output from the LSTM layer is then directly passed through a fully-connected linear layer, followed by a sigmoid activation function. This final output represents the probability distribution $P(\psi)$, providing a probabilistic estimate of the human driver's driving style. The module is trained to minimize the binary cross-entropy loss between its output and the corresponding labels.

Rationality Inference Module: The rationality inference module follows a similar training procedure, utilizing input data $\{x(i), u_h(i), \psi\}_{i=t-N_{seq}}^t$ and corresponding labels denoted as β , all sourced from the same datasets D_{train} . In order to unveil the relationships concealed within the historical trajectories, we once again employ an LSTM layer. Subsequently, to compute both the mean μ_β and variance Σ_β of the rationality coefficient, we establish connections to two linear layers integrated with the LSTM layer. The first linear layer is linked to a sigmoid activation function, enabling us to compute μ_β . Conversely, the second linear layer is connected to a Rectified Linear Unit (ReLU) activation function, enabling the calculation of Σ_β . The module is trained to minimize the negative log-likelihood loss between its output and the corresponding labels.

Both modules are trained using the Adam optimization algorithm [30] with a learning rate 0.00001. These trained modules are employed to make probabilistic inferences on human driving style and rationality based on real-time observations.

B. Planning-based Human Motion Prediction

Once the internal states are inferred, we can compute the probability distribution of human motion for Eq.(3d). However, deriving its analytical expression is challenging, so we adopt the Laplace Approximation [15]. As a result, the probability of predicted human motion can be represented by normal distribution as $P(u_h^k|x^k, u_r^k, \psi, \beta) = \mathcal{N}(\mu_{u_h}^k(x^k, u_r^k), \Sigma_{u_h}^k(x^k, u_r^k))$ for $k = 0, \dots, N-1$. These mean and covariance are respectively described by:

$$\begin{aligned} \mu_{u_h}^k(x^k, u_r^k) &= \arg \max_{u_h^k} R_h^\psi(x^k, u_r^k, u_h^k), \\ \Sigma_{u_h}^k(x^k, u_r^k) &= -[\nabla^2 \exp(\beta R_h^\psi(x^k, u_r^k, u_h^k))|_{u_h^k=\mu_{u_h}^k(x^k, u_r^k)}]^{-1} \\ &= -[\nabla^2 \exp(R_h^\psi(x^k, u_r^k, u_h^k))|_{u_h^k=\mu_{u_h}^k(x^k, u_r^k)}]^{-1}/\beta \\ &= \Sigma_{u_h^\psi}^k(x^k, u_r^k)/\beta. \end{aligned} \quad (5)$$

where $\Sigma_{u_h^\psi}^k(x^k, u_r^k)$ is the baseline covariance with respect to human driving style. Finally, given the inferred driving style $\bar{\psi}$ and rationality coefficient μ_β , the probability distribution of human motion is rewritten as:

$$P(u_h^k|x^k, u_r^k, \bar{\psi}, \mu_\beta) = \mathcal{N}(\mu_{u_h}^k(x^k, u_r^k), \Sigma_{u_h^\psi}^k(x^k, u_r^k)/\mu_\beta). \quad (6)$$

C. Active Motion Planning of Autonomous Vehicle

Given the probability distribution of human motion, autonomous vehicle aims to solve Eq.(3). However, this uncertainty introduces a high-dimensional stochastic component to the optimization problem, resulting in a significant increase in computational demands. We present a solution to this issue by introducing a sampling-based motion planning algorithm inspired by the Model Predictive Path Integral (MPPI) [31]. The active motion planning algorithm involves four main submodules: (1) sampling autonomous vehicle motion; (2) sampling human motion; (3) future probability computation; and (4) evaluation and selection.

Sampling Autonomous Vehicle Motion: At time step t , we commence the algorithm with the current state $x(t)$,

probability over driving style $P(\psi)$, and inferred rationality coefficient μ_β as initial inputs. The first step involves generating K_r parallel samples of \mathbf{u}_r , which are drawn from a uniform distribution specified as follows:

$$\mathbf{u}_r^i \sim \mathcal{U}(u_{\min}, u_{\max}), \quad \forall i = 0, 1, \dots, K_r - 1$$

where u_{\min} and u_{\max} denote the constraints imposed on the motions.

Sampling Human Motion: Given $P(\psi)$, $K_r \times K_h$ potential driving styles are sampled as follows:

$$\begin{aligned} \bar{\psi}^{i,j} &\sim P(\psi), \quad \forall i = 0, 1, \dots, K_r - 1, \\ &\quad \forall j = 0, 1, \dots, K_h - 1. \end{aligned}$$

Consequently, we can compute the probability distribution of human motions with respect to the sampled \mathbf{u}_r^i and $\bar{\psi}^{i,j}$ using Eq.(6). Then, human motion $u_h^{i,j,k}$ is drawn from this probability distribution at each time step k as follows:

$$u_h^{i,j,k} \sim \mathcal{N}(\mu_{u_h}^k(x^{i,j,k}, u_r^{i,k}), \Sigma_{u_h}^k(x^{i,j,k}, u_r^{i,k}) / \mu_\beta). \quad (7)$$

Once $u_r^{i,k}$ and $u_h^{i,j,k}$ are sampled, the algorithm proceeds by iteratively updating the next state $x^{i,j,k+1}$ for every time step $k = 0, \dots, N - 1$ with Eq.(1):

$$x^{i,j,k+1} = f(x^{i,j,k}, u_r^{i,k}, u_h^{i,j,k})$$

where $x^{i,j,0} = x(t)$.

Future Probability Computation: To incorporate active inference into our approach, we utilize the trained driving style inference module to compute the future probability distribution over human driving styles, denoted as $P(\bar{\psi}^{i,j,k})$. This probability is estimated based on the predicted human motions $u_h^{i,j,k}$ and state $x^{i,j,k}$. Then, we compute the product of probabilities over the N time steps as follows:

$$P(\bar{\psi}^{i,j}) = \prod_{k=0}^{N-1} P(\bar{\psi}^{i,j,k}). \quad (8)$$

This $P(\bar{\psi}^{i,j})$ plays a crucial role in influencing the motions of autonomous vehicle. It acts as a weight for \mathbf{u}_r^i , effectively encouraging the vehicle to actively adapt to and anticipate the most probable human internal states.

Evaluation and Selection: The final step in motion planning is to select the optimal input sequence \mathbf{u}_r^* from all sampled \mathbf{u}_r^i . The goal of the autonomous vehicle is to choose \mathbf{u}_r^* that strikes a balance between ensuring safety against uncertainty in human motion and active inference while considering the autonomous vehicle's reward. We first identify the samples that violate the constraints Eq.(3e)-(3f). To account for the uncertain human motion, we update the safety boundary for Eq.(3f) using Eq.(4), and then retain only those samples that satisfy the safety criteria as follows:

$$\begin{aligned} \Omega_r &= \{i | x^{i,j,k}, u_r^{i,k}, u_h^{i,j,k} \text{ satisfy Eq.(3e) - (3f)}, \forall j, k\}, \\ \Omega_h &= \{j | x^{i,j,k}, u_r^{i,k}, u_h^{i,j,k} \text{ satisfy Eq.(3e) - (3f)}, \forall i, k\}. \end{aligned} \quad (9)$$

Next, we calculate the expected reward $R_r^{i,j}$ using Eq.(3a), considering all sampled motions of both vehicles. Then, \mathbf{u}_r^*

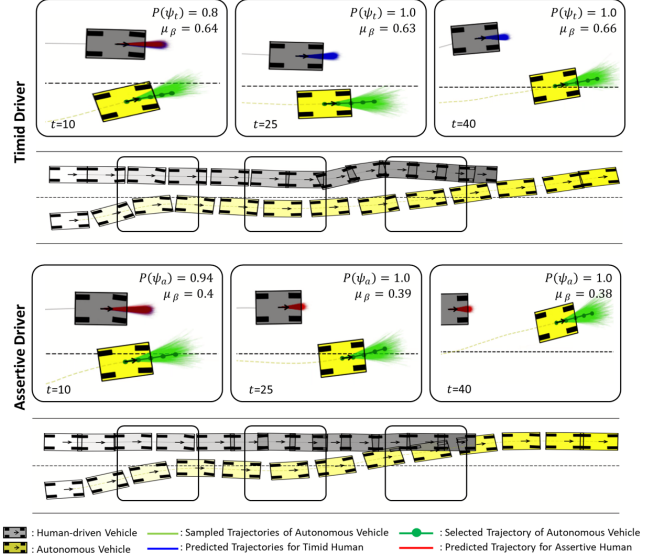


Fig. 4. Simulation snapshots in a lane change scenario: the autonomous vehicle interacts with a human driver whose true internal states are (top) $\psi = \psi_t$ and $\beta = 0.62$; and (bottom) $\psi = \psi_a$ and $\beta = 0.36$.

is computed by taking a reward-weighted average over \mathbf{u}_r^i with Eq.(8) and (9) as follows:

$$\begin{aligned} \mathbf{u}_r^* &= \frac{1}{\zeta_1} \sum_{i \in \Omega_r} \zeta_2^i \mathbf{u}_r^i \\ \zeta_1 &= \sum_{i \in \Omega_r} \zeta_2^i \\ \zeta_2^i &= \frac{1}{|\Omega_h|} \sum_{j \in \Omega_h} P(\bar{\psi}^{i,j}) \exp\left(-\frac{1}{\eta} (R_r^{i,j} - R_r^{\min})\right) \end{aligned}$$

where $R_r^{\min} := \min R_r^{i,j}$ represents the minimum expected cost, and η is a hyperparameter that controls the degree of selectiveness in the weighted average.

V. NUMERICAL SIMULATION

A. Implementation Details

To assess the performance of the proposed algorithm, we investigate a lane change scenario where an autonomous vehicle safely merges into the left lane while interacting with an uncertain human driver.

Simulated Human Decision Model: The human decide their motions with an underlying true reward function R_ψ with rationality coefficient β . The weight parameter set of reward $\theta_\psi^i := [\theta_{\psi,1}, \theta_{\psi,2}, \theta_{\psi,3}]$ varies with each driving style, and R_h^ψ is then modeled using the corresponding weight parameter set as follows:

$$R_h^\psi = \theta_{\psi,1} R_{ref} + \theta_{\psi,2} R_{input} + \theta_{\psi,3} R_{safe}$$

Here, R_{ref} represents the quadratic cost for penalizing deviations from the reference state, R_{input} is the quadratic cost for penalizing input efforts, and R_{safe} is the collision avoidance cost, penalizing instances when the distance between vehicles falls below the safe distance. We consider two distinct

TABLE I
PERFORMANCE STATISTICS OF INTERNAL STATE INFERENCE

	Timid Human	Assertive Human
Accuracy of ψ	85%	98%
RMSE of β	0.1	0.09

driving styles in the simulation, namely timid and assertive, respectively denoted by ψ_t and ψ_a . They in general differs in reaction to autonomous vehicle, i.e., the timid driver reacts to avoid a collision with the autonomous vehicle, while the assertive driver ignores the autonomous vehicle’s motion. To distinguish between these reactions, we set the weight for the collision avoidance cost as zero. In each scenario, the true human rationality coefficient is randomly drawn within the range $0.2 < \beta < 1$. With R_ψ and β , humans randomly choose noisy motions based on Nash equilibrium [32].

Simulation Set-up: All simulations are executed by a desktop computer with an AMD Ryzen 7 3700X 8-Core processor with 32GB RAM and a Nvidia GeForce RTX 2060 GPU. To train and test the inference module, we generate datasets by executing 15,000 simulations for each driving style, with the true β randomly sampled from the range of 0.2 to 1. The trajectory of each simulation is collected over $N_{sim} = 60$ and split into $N_{seq} = 5$. The proposed motion planning is formulated with a discrete time step $\Delta t = 0.2s$, $N = 5$, and $K_r = 500$ and $K_h = 3$ for sampling autonomous vehicle and human motions. Further details of the simulation set-up can be found in our GitHub repository: <https://github.com/HMCL-UNIST/IntegratedMotionPrediction.git>.

Comparative Analysis: The comparative analysis is conducted with two existing prediction approaches: (1) the planning-based prediction, which utilizes Bayesian inference with discretized rationality coefficients ($\beta \in \{0.2, 1\}$) [10], [19]; and (2) the data-driven prediction, which directly learns human future trajectories based on a Conditional Variational AutoEncoder (CVAE) [6]. The CVAE is constructed using LSTM layers for the encoder and decoder. Both existing approaches employ passive inference without active planning.

B. Simulation Results

We have conducted two case studies: interaction with (1) the human driver that exhibits a driving style consistent with the trained model (timid/assertive); and (2) the human driver with a driving style that deviates from the trained datasets (untrained). For each driving style, we run 500 simulations and test the algorithm.

Case Study 1: Fig. 4 shows the snapshots from the simulation with the proposed algorithm. Initially, human future trajectories are sampled in both driving styles due to a lack of specific information about the driver’s style. However, as time progresses, the algorithm enables it to accurately sample future trajectories according to inferred $P(\psi)$ and β .

Table. I presents the average performance of the proposed internal state inference modules. The accuracy of ψ is represented by the percentage at which the autonomous vehicle

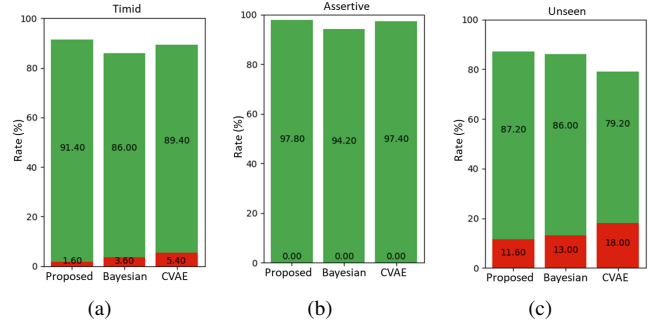


Fig. 5. The average collision rates (*red*) and success rates (*green*) within the simulation time, when the true human model has (a) timid, (b) assertive, and (c) untrained driving style.

correctly identifies the human driving style. To assess the accuracy of β , we utilize the Root Mean Square Error (RMSE) metric. This table highlights the algorithm’s reliability in inferring both human driving style and rationality.

In Fig. 5(a-b), we provide a comparison between our proposed algorithm and two existing approaches. This comparison assesses both collision rates and success rates throughout the simulations. The success rates represent the frequency of successful lane changes completed by the autonomous vehicle within the simulation duration. Our proposed method outperforms the existing ones in terms of planning performance, specifically exhibiting a significantly lower collision rate and a higher success rate. These results emphasize the importance of considering human rationality and active inference to safely achieve the motion planning goal.

Case Study 2: We investigate scenarios where the autonomous vehicle lacks prior knowledge of the true human driving style. To emulate such situations, we define the untrained driving style using reward weights that significantly differ from the two trained driving styles. Even in cases where the true human driving style is outside the autonomous vehicle’s prior knowledge, as depicted in Fig. 5(c), the proposed algorithm effectively manages these situations by effectively adjusting the level of rationality, ensuring safe operation even when faced with an untrained driving style.

VI. CONCLUSIONS

In this work, we proposed a unified prediction and planning algorithm for an autonomous vehicle to interact with a human-driven vehicle having uncertain internal states, i.e., driving style and rationality. Coping with the uncertainties induced by these internal states, the proposed prediction method incorporates LSTM-based internal state inference and planning-based prediction. Subsequently, we employ a sampling-based SMPC to simultaneously accomplish the autonomous vehicle’s navigation goal and active inference on human internal states. The proposed method is demonstrated to enhance the planning performance by delivering reliable predictions in lane change scenarios. Future works will further enhance the fidelity of the proposed algorithm by training the inference module and diversifying human internal states using real human driving data.

REFERENCES

- [1] D. E. Bentrachou, S. Glaser, M. Elhenawy, and A. Rakotonirainy, "Use of social interaction and intention to improve motion prediction within automated vehicle framework: A review," *IEEE Transactions on Intelligent Transportation Systems*, 2022.
- [2] C. Laugier, I. E. Paromtchik, M. Perrollaz, M. Yong, J.-D. Yoder, C. Tay, K. Mekhnacha, and A. Nègre, "Probabilistic analysis of dynamic scenes and collision risks assessment to improve driving safety," *IEEE Intelligent Transportation Systems Magazine*, vol. 3, no. 4, pp. 4–19, 2011.
- [3] A. Zyner, S. Worrall, J. Ward, and E. Nebot, "Long short term memory for driver intent prediction," in *2017 IEEE Intelligent Vehicles Symposium (IV)*. IEEE, 2017, pp. 1484–1489.
- [4] P. Kumar, M. Perrollaz, S. Lefevre, and C. Laugier, "Learning-based approach for online lane change intention prediction," in *2013 IEEE Intelligent Vehicles Symposium (IV)*. IEEE, 2013, pp. 797–802.
- [5] Y. Yoon, C. Kim, J. Lee, and K. Yi, "Interaction-aware probabilistic trajectory prediction of cut-in vehicles using gaussian process for proactive control of autonomous vehicles," *IEEE Access*, vol. 9, pp. 63 440–63 455, 2021.
- [6] E. Schmerling, K. Leung, W. Vollprecht, and M. Pavone, "Multimodal probabilistic model-based planning for human-robot interaction," in *2018 IEEE International Conference on Robotics and Automation (ICRA)*. IEEE, 2018, pp. 3399–3406.
- [7] N. Kaempchen, K. Weiss, M. Schaefer, and K. C. Dietmayer, "Imm object tracking for high dynamic driving maneuvers," in *IEEE Intelligent Vehicles Symposium, 2004*. IEEE, 2004, pp. 825–830.
- [8] J. F. Fisac, E. Bronstein, E. Stefansson, D. Sadigh, S. S. Sastry, and A. D. Dragan, "Hierarchical game-theoretic planning for autonomous vehicles," in *2019 International conference on robotics and automation (ICRA)*. IEEE, 2019, pp. 9590–9596.
- [9] W. Schwarting, A. Pierson, J. Alonso-Mora, S. Karaman, and D. Rus, "Social behavior for autonomous vehicles," *Proceedings of the National Academy of Sciences*, vol. 116, no. 50, pp. 24 972–24 978, 2019.
- [10] D. Fridovich-Keil, A. Bajcsy, J. F. Fisac, S. L. Herbert, S. Wang, A. D. Dragan, and C. J. Tomlin, "Confidence-aware motion prediction for real-time collision avoidance," *The International Journal of Robotics Research*, vol. 39, no. 2-3, pp. 250–265, 2020.
- [11] D. Sadigh, N. Landolfi, S. S. Sastry, S. A. Seshia, and A. D. Dragan, "Planning for cars that coordinate with people: leveraging effects on human actions for planning and active information gathering over human internal state," *Autonomous Robots*, vol. 42, pp. 1405–1426, 2018.
- [12] H. Hu and J. F. Fisac, "Active uncertainty reduction for human-robot interaction: An implicit dual control approach," in *International Workshop on the Algorithmic Foundations of Robotics*. Springer, 2022, pp. 385–401.
- [13] T. Zhang, W. Song, M. Fu, Y. Yang, and M. Wang, "Vehicle motion prediction at intersections based on the turning intention and prior trajectories model," *IEEE/CAA Journal of Automatica Sinica*, vol. 8, no. 10, pp. 1657–1666, 2021.
- [14] A. Rudenko, L. Palmieri, M. Herman, K. M. Kitani, D. M. Gavrila, and K. O. Arras, "Human motion trajectory prediction: A survey," *The International Journal of Robotics Research*, vol. 39, no. 8, pp. 895–935, 2020.
- [15] S. Levine and V. Koltun, "Continuous inverse optimal control with locally optimal examples," *arXiv preprint arXiv:1206.4617*, 2012.
- [16] L. Sun, W. Zhan, and M. Tomizuka, "Probabilistic prediction of interactive driving behavior via hierarchical inverse reinforcement learning," in *2018 21st International Conference on Intelligent Transportation Systems (ITSC)*. IEEE, 2018, pp. 2111–2117.
- [17] W.-C. Ma, D.-A. Huang, N. Lee, and K. M. Kitani, "Forecasting interactive dynamics of pedestrians with fictitious play," in *Proceedings of the IEEE Conference on Computer Vision and Pattern Recognition*, 2017, pp. 774–782.
- [18] B. Zhou, W. Schwarting, D. Rus, and J. Alonso-Mora, "Joint multi-policy behavior estimation and receding-horizon trajectory planning for automated urban driving," in *2018 IEEE International Conference on Robotics and Automation (ICRA)*. IEEE, 2018, pp. 2388–2394.
- [19] H. Hu, K. Nakamura, and J. F. Fisac, "Sharp: Shielding-aware robust planning for safe and efficient human-robot interaction," *IEEE Robotics and Automation Letters*, vol. 7, no. 2, pp. 5591–5598, 2022.
- [20] R. Tian, L. Sun, M. Tomizuka, and D. Isele, "Anytime game-theoretic planning with active reasoning about humans' latent states for human-centered robots," in *2021 IEEE International Conference on Robotics and Automation (ICRA)*. IEEE, 2021, pp. 4509–4515.
- [21] C. Brooks and D. Szafir, "Balanced information gathering and goal-oriented actions in shared autonomy," in *2019 14th ACM/IEEE International Conference on Human-Robot Interaction (HRI)*. IEEE, 2019, pp. 85–94.
- [22] H. Song, D. Luan, W. Ding, M. Y. Wang, and Q. Chen, "Learning to predict vehicle trajectories with model-based planning," in *Conference on Robot Learning*. PMLR, 2022, pp. 1035–1045.
- [23] Y. Hu, W. Zhan, L. Sun, and M. Tomizuka, "Multi-modal probabilistic prediction of interactive behavior via an interpretable model," in *2019 IEEE Intelligent Vehicles Symposium (IV)*. IEEE, 2019, pp. 557–563.
- [24] M. Meghji, Y. Luo, Q. H. Ho, P. Cai, S. Verma, D. Rus, and D. Hsu, "Context and intention aware planning for urban driving," in *2019 IEEE/RSJ International Conference on Intelligent Robots and Systems (IROS)*. IEEE, 2019, pp. 2891–2898.
- [25] L. Li, W. Zhao, C. Xu, C. Wang, Q. Chen, and S. Dai, "Lane-change intention inference based on rnn for autonomous driving on highways," *IEEE Transactions on Vehicular Technology*, vol. 70, no. 6, pp. 5499–5510, 2021.
- [26] R. Rajamani, *Vehicle dynamics and control*. Springer Science & Business Media, 2011.
- [27] C. L. Baker, J. B. Tenenbaum, and R. R. Saxe, "Goal inference as inverse planning," in *Proceedings of the Annual Meeting of the Cognitive Science Society*, vol. 29, no. 29, 2007.
- [28] W. Schwarting, J. Alonso-Mora, L. Pauli, S. Karaman, and D. Rus, "Parallel autonomy in automated vehicles: Safe motion generation with minimal intervention," in *2017 IEEE International Conference on Robotics and Automation (ICRA)*. IEEE, 2017, pp. 1928–1935.
- [29] W. Wang, J. Xi, and D. Zhao, "Driving style analysis using primitive driving patterns with bayesian nonparametric approaches," *IEEE Transactions on Intelligent Transportation Systems*, vol. 20, no. 8, pp. 2986–2998, 2018.
- [30] D. P. Kingma and J. Ba, "Adam: A method for stochastic optimization," *arXiv preprint arXiv:1412.6980*, 2014.
- [31] G. Williams, P. Drews, B. Goldfain, J. M. Rehg, and E. A. Theodorou, "Aggressive driving with model predictive path integral control," in *2016 IEEE International Conference on Robotics and Automation (ICRA)*. IEEE, 2016, pp. 1433–1440.
- [32] D. Fridovich-Keil, E. Ratner, L. Peters, A. D. Dragan, and C. J. Tomlin, "Efficient iterative linear-quadratic approximations for nonlinear multi-player general-sum differential games," in *2020 IEEE international conference on robotics and automation (ICRA)*. IEEE, 2020, pp. 1475–1481.